Accepted Manuscript

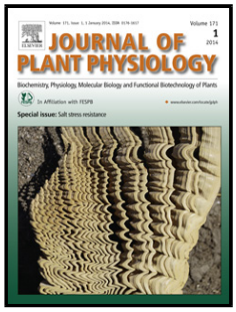

Title: Antioxidative response in variegated *Pelargonium zonale* leaves and generation of extracellular H_2O_2 in (peri)vascular tissue induced by sunlight and paraquat

Author: Marija Vidović Filis Morina Ljiljana Prokić Sonja Milić-Komić Bojana Živanović Sonja Veljović Jovanović

PII: S0176-1617(16)30178-X
DOI: http://dx.doi.org/doi:10.1016/j.jplph.2016.07.017
Reference: JPLPH 52434

To appear in:

Received date: 14-3-2016
Revised date: 19-7-2016
Accepted date: 20-7-2016

Please cite this article as: Vidović Marija, Morina Filis, Prokić Ljiljana, Milić-Komić Sonja, Živanović Bojana, Jovanović Sonja Veljović.Antioxidative response in variegated Pelargonium zonale leaves and generation of extracellular H2O2 in (peri)vascular tissue induced by sunlight and paraquat.*Journal of Plant Physiology* http://dx.doi.org/10.1016/j.jplph.2016.07.017

Antioxidative response in variegated *Pelargonium zonale* leaves and generation of extracellular H_2O_2 in (peri)vascular tissue induced by sunlight and paraquat

Marija Vidović[a], Filis Morina[a], Ljiljana Prokić[b], Sonja Milić-Komić[a], Bojana Živanović[a] and Sonja Veljović Jovanović[a*]

[a]*Department of Life Sciences, Institute for Multidisciplinary Research, University of Belgrade, Kneza Višeslava 1, 11030, Belgrade, Serbia*

[b]*Faculty of Agriculture, University of Belgrade, Nemanjina 6, 11080 Belgrade, Serbia*

*Corresponding author:
dr Sonja Veljović Jovanović,
email sonjavel@imsi.rs
Department of Life Sciences, Institute for Multidisciplinary Research, University of Belgrade, Kneza Višeslava 1, 11030, Belgrade, Serbia
fax. +381113055289
phone +381113555258

E-mail addresses: marija@imsi.rs (M.V.), filkis14@hotmail.com (F.M.), ljprokic@agrif.bg.ac.rs (Lj.P.), soonjam@gmail.com (S.M.), bokazivanovic@yahoo.com (B.Ž.), sonjavel@imsi.rs (S.V.J).

Abstract/Summary

In this study we exposed variegated leaves of *Pelargonium zonale* to strong sunlight (>1100 μmol m^{-2} s^{-1} of photosynthetically active radiation) with and without paraquat (Pq), with the aim to elucidate the mechanisms of H_2O_2 regulation in green and white tissues with respect to the photosynthetically-dependent generation of reactive oxygen species (ROS). Sunlight induced marked accumulation of H_2O_2 in the apoplast of vascular and (peri)vascular tissues only in green sectors. This effect was enhanced by the addition of Pq. In the presence of diphenyl iodide, an NADPH oxidase inhibitor, H_2O_2 accumulation was abolished. Two tissues had distinct light-induced responses: in photosynthetic cells, sunlight rapidly provoked ascorbate (Asc) biosynthesis and an increase of glutathione reductase (GR) and catalase activities, while in non-photosynthetic cells, early up-regulation of soluble ascorbate peroxidase, dehydroascorbate reductase (DHAR) and GR activities was observed. Paraquat addition stimulated DHAR and GR activities in green sectors, while in white sectors activities of monodehydroascorbate reductase, DHAR and class III peroxidases, as well as Asc rapidly increased. We discuss differential antioxidative responses in the two tissues in the frame of their contrasting metabolisms, and the possible role of (peri)vascular H_2O_2 in signaling.

Abbreviations:

ABA, abscisic acid; APX, ascorbate peroxidase; Asc, reduced ascorbate; CAT, catalase; DAB, 3,3'-diaminobenzidine; DHA, dehydroascorbate; DHAR, dehydroascorbate reductase; GR, glutathione reductase; GSH, reduced glutathione; GSSG, oxidized form of glutathione; HPLC, high-performance liquid chromatography; MDAR, monodehydroascorbate reductase; $O_2^{\bullet -}$, superoxide anion radical; PAR, photosynthetically active radiation (400-700 nm); PODs, class III peroxidases; PS, photosystem; ROS, reactive oxygen species; RsA, redox state of ascorbate; RsG, redox state of glutathione; Pq, paraquat (methyl viologen); SDS-PAGE, sodium dodecylsulphate polyacrylamide gel electrophoresis; SOD, superoxide dismutase.

Key words

Abscisic acid, ascorbate-glutathione cycle, strong light, hydrogen peroxide, paraquat, variegated plants.

1. Introduction

In green leaves, the photosynthetic electron transport chain and photorespiration are the main sources of reactive oxygen species (ROS), even under optimal growth conditions (Foyer and Shigeoka, 2011). In addition to photosynthetic tissue, green-white variegated plants (such as *Pelargonium zonale*) have non-photosynthetic tissue lacking functional chloroplasts and peroxisomes (Vidović et al., 2015). Therefore, in this tissue, the most important sources of ROS generation are the mitochondrial electron transport chain and apoplast (Møller, 2001; Sierla et al., 2013). However, the respiration rate in non-photosynthetic leaf tissue of variegated *P. zonale* was significantly lower compared to the photosynthetic tissue (Toshoji et al., 2011).

In our previous studies, we have characterized two different antioxidative systems in photosynthetic and non-photosynthetic leaf tissues of *P. zonale* (Vidović et al., 2016; 2015). Non-photosynthetic tissue had constitutively higher activities of enzymes involved in ascorbate-glutathione (Asc-GSH) cycle and Cu/Zn superoxide dismutase (SOD) compared to the photosynthetic tissue. Moreover, higher cytosolic ascorbate and total cellular glutathione contents in non-photosynthetic cells compared to the photosynthetic ones were observed. Photosynthetic tissue is distinguished from non-photosynthetic tissue by higher total ascorbate content as well as higher catalase (CAT) and thylakoid ascorbate peroxidase (APX) activities. Under optimal growth conditions, photosynthetic tissue contained higher level of carbonylated proteins than non-photosynthetic tissue, which was even more pronounced under high light, confirming more intensive pro-oxidative conditions in this tissue type (Vidović et al., 2015).

High light intensity accelerates superoxide anion radical ($O_2^{\bullet-}$) generation at photosystem I (PS I) through reduction of molecular oxygen in the Mehler reaction (Asada, 2006). In addition to high light, the herbicide paraquat (Pq, known as methyl viologen) is commonly used to induce oxidative stress in chloroplasts through predominant acceleration of the Mehler reaction (Neuhaus and Stitt, 1989; Kangasjärvi et al., 2008; Scarpeci et al., 2008; Stonebloom et al., 2012). In addition to its toxicity to chloroplasts, Pq^{2+} is also toxic to mitochondria (but to a lesser extent), since it can be reduced by electrons "leaking" from complex I, and therefore impair the redox homeostasis in these organelles (Asada, 2000; Vicente et al., 2001; Cochemé and Murphy, 2008, Lascano et al., 2012). Intensive Pq treatment (prolonged application or higher concentrations) can result in severe membrane damage and cell death (Li et al., 2013).

In this study, we investigated the dynamics of Asc-GSH cycle components, CAT and class III peroxidases (POD) in variegated *P. zonale* leaves during a 9-h period under increased

cellular H_2O_2 availability. Considering that photosynthetic and non-photosynthetic leaf cells have different constitutive H_2O_2 regulating systems under optimal growth conditions, we expected that the two tissues would have distinct responses to oxidative stress induced by light excess and the pro-oxidative agent, Pq. We hypothesized that accumulation of H_2O_2 would be higher in photosynthetic tissue due to increased ROS generation dependent from photosynthesis. Furthermore, we examined whether photosynthetically derived H_2O_2 accumulation might be involved in intercellular signaling between photosynthetic and non-photosynthetic leaf tissue.

2. Material and methods

2.1. Plant material and experimental conditions

The variegated *Pelargonium zonale* cv. "Ben Franklin" plants were purchased from Fir Trees Pelargonium (Stokesley, North Yorkshire, UK) nursery. Plants were grown and propagated under 250 μmol m^{-2} s^{-1} of photosynthetically active radiation (PAR, 400-700 nm) under 14/10 h day/night photoperiod, 26/18ºC day/night temperatures and relative humidity of 60-70%. This cultivar is a periclinal chimera with white leaf margins, caused by the lack of functional chloroplasts in L2 and L3 cell layers (hypodermis and mesophyll), while chloroplasts were observed in the guard cells in L1 layer (epidermis) (Vidović et al., 2016).

For controls, separated white and green areas of dark adapted leaves (four fully developed leaves per plant, four plants in total) were immediately frozen in liquid nitrogen and stored at −80ºC until analysis. Further, three dark adapted leaves per plant from ten plants in total were excised at the base of stems with a razor blade, and one half was placed in 1.5 mL tubes covered with Alu foil filled with water, and the other half in 100 μM Pq solution in water. All leaves were exposed to direct solar radiation over 9 h on a clear, sunny day, when maximal PAR was almost 2000 μmol m^{-2} s^{-1} at noon (Fig. A1), which exceeds the intensity required for achieving maximal net CO_2 assimilation rate (400 μmol m^{-2} s^{-1}, light curves are not shown).

The dynamics of the responses of antioxidants in *P. zonale* leaves treated with Pq were monitored in relation to only sunlight exposed leaves and dark adapted leaves. The amount of Pq taken up by the whole leaf was calculated by measuring the volume of remained solution per leaf. The average amounts of Pq in the whole leaf were: 16.2 ± 1.6; 120.4 ± 7.0; 262.9 ± 20.9

nmol g^{-1}_{FW}, after the 1st, the 4th and the 9th h of exposure, respectively. The experiments were repeated three times in the period from June to September.

2.2. Ascorbate and glutathione redox status analysis

Measurements of reduced ascorbate (Asc), dehydroascorbate (DHA), reduced and oxidized glutathione (GSH and GSSH) contents in the photosynthetic and non-photosynthetic leaf tissue were performed by high-performance liquid chromatography (HPLC, Shimadzu LC-20AB Prominence liquid chromatograph, Shimadzu, Kyoto, Japan) as described by Vidović et al. (2015). The redox state of ascorbate (RsA) was calculated as a percentage of Asc in total ascorbate (Asc + DHA) content, while the redox state of glutathione (RsG) was calculated as: 100% × [GSH/(GSH + 2GSSG)].

2.3. Enzyme extractions and assays

Extraction of soluble ascorbate peroxidase (APX, EC 1.11.1.11), monodehydroascorbate reductase (MDAR, EC 1.6.5.4), dehydroascorbate reductase (DHAR, EC 1.8.5.1), glutathione reductase (GR, EC 1.8.1.7), class III peroxidases (PODs, EC 1.11.1.7), catalase (CAT, EC 1.11.1.6) and superoxide dismutase (SOD, EC 1.15.1.1) was performed as reported previously (Vidović et al., 2016).

The activities of antioxidative enzymes were determined spectrophotometrically, in triplicates, using a temperature-controlled spectrophotometer (Shimadzu, UV-160, Kyoto, Japan), as described in our previous study (Vidović et al., 2016).

2.4. SDS-PAGE and SOD gel blot analysis

For SOD gel blot analysis, 7 µg of total soluble proteins of green and white leaf extracts were separated by SDS-PAGE (15% gel) and electrotransferred to a polyvinylidene difluoride membrane according to Vidović et al. (2016). For Cu/Zn SOD detection primary antiserum: rabbit anti-Arabidopsis chloroplastic Cu/ZnSOD (CSD2) antiserum (AS06 170, Agrisera) (diluted 1:1000) was used. Equal loading was confirmed by staining the replicate gels with silver.

2.5. Detection of accumulated H_2O_2

Detection of H_2O_2 was based on the 3,3'-diaminobenzidine (DAB) 'up-take' method according to Fryer et al. (2003). After exposing leaves to high light (1100 ± 100 μmol m^{-2} s^{-1}) and 100 μM Pq for 1 h (at least twenty variegated leaves, from ten plants in total per treatment), they were placed in tubes filled with solution of 1 mg mL^{-1} DAB in 100 mM sodium acetate buffer (pH 3.8) and returned to the same light irradiance. After 1 h, leaves were cleared in boiling 70% (v/v) ethanol (for 10 min) with 10% glycerol. The same results were obtained when leaves were incubated in DAB (with and without Pq) immediately upon light exposure. In addition, different leaf morphotypes, sectorial chimeras, totally green and totally white leaves were used. As a negative control, detached leaves were placed in the buffer solution containing no DAB, and after chlorophyll removal they showed no brown precipitate. Only leaves that absorbed equal amounts of DAB (350 ± 25 μg g^{-1}_{FW} on average) were analyzed. Each leaf was photographed before and after chlorophyll removal, and high resolution images were made using an Olympus BX41light microscope equipped with Olympus C7070 camera (Olympus Optical Co., Hamburg, Germany).

Densitometric analysis of H_2O_2 accumulation was performed using ImageJ software 1.45 version (http://imagej.nih.gov/ij/) similar to the method described by Morina et al. (2016). Accumulation of H_2O_2, measured as staining intensity is presented in arbitrary units.

In order to determine the site and source of H_2O_2 generation, we incubated leaves for 1 h under high light in 0.1 mM diphenyl iodide (DPI), a NADPH oxidase inhibitor, in solution containing exogenous ABA (0.1 mM) and in solution containing 50 U of exogenous CAT (from bovine liver) (similarly as described in Hu et al., 2006). The efficiency of ABA and CAT absorption by leaves was confirmed. In total, ten leaves for each pre-treatment were used. After pre-treatment, leaves were incubated in DAB solution as described above.

2.6. Measurements of stomatal conductance

Direct readout of stomatal conductance (g_s) was done using a porometer (AP4, Delta-T, Cambridge, U.K.). Recordings were done on photosynthetic and non-photosynthetic tissue from fully developed leaves exposed to different treatments. For each treatment, three leaves per plant (four plants in total) were used.

2.7. Abscisic acid determination

For ABA content determination, leaves were separated to: 1. white sectors (non-photosynthetic tissue), 2. (peri)vascular tissue which consisted of several main veins, all extending from the leaf petiole from green sectors, and 3. to the rest of green sectors (photosynthetic tissue), similarly as described in Kuźniak et al. (2016). ABA content was determined by indirect enzyme-linked immunosorbent assay (ELISA) following the procedure described in Morina et al. (2016). Three fully developed leaves per seven plants per treatment were detached and exposed to growth light (250 μmol m^{-2} s^{-1} PAR), high light (1100 ± 100 μmol m^{-2} s^{-1} PAR) or 100 μM Pq for 1 h. In addition, samples from dark adapted leaves were collected. Finally, all three leaves originating from the same plant were pooled together (tissues were separated) and analyzed.

2.8. Statistical analysis

The significance of tissue type effect on enzyme activities, ascorbate and glutathione pools, as well as significant differences in antioxidants' levels between dark adapted leaves (control), and 1 h, 4 h and 9 h of sunlight and Pq exposure, in photosynthetic and non-photosynthetic leaf tissues, separately, were tested by the Mann-Whitney U test. Tukey's post hoc test was used to test for significant differences of stomatal conductance and ABA contents among treatment groups for each tissue type. Both tests were conducted with IBM SPSS statistics software (Version 20.0, SPSS Inc., Chicago, USA). The significance threshold value was set at 0.05.

3. Results

3.1. The effect of sunlight and Pq on Asc and GSH leaf content

In the dark adapted leaves, Asc contents were similar in both tissue types, while higher ascorbate redox state (RsA) was detected in the photosynthetic tissue compared to the non-photosynthetic one (Fig. 1).

Upon sun exposure, both Asc and DHA levels doubled rapidly (within the 1^{st} h) in photosynthetic cells, and the RsA remained unchanged. Asc content decreased over time and after 9 h it reached the same level as in dark adapted leaves (for statistical significance see Table A1). The initial stimulation of Asc biosynthesis in photosynthetic cells was omitted under Pq treatment, without changes in RsA. Non-photosynthetic cells responded to sunlight exposure by

rapid Asc oxidation, which was recovered after 4 h. On the contrary, Pq addition suppressed the initial increase of DHA content in the same tissue, and provoked an increase of Asc content (Fig. 1; Table A1).

Fig. 1.

In the dark adapted plants, non-photosynthetic cells had three-fold higher content of GSH and two times higher glutathione redox state (RsG) compared to the photosynthetic ones (Fig. 2; Table A2). This tissue-specific glutathione distribution was also observed under optimal light conditions, in which the total glutathione content was about two-fold higher in non-photosynthetic compared to photosynthetic cells (Vidović et al., 2016).

Fig. 2.

Both strong sunlight and Pq induced a similar transient GSH increase within 1 h in photosynthetic cells, accompanied by 3-fold decrease of GSSG (compared to respective controls; Fig. 3, Table A2). In non-photosynthetic tissue, however, GSSG content slightly increased under sunlight, while a rapid three-fold increase was observed with Pq. Accordingly, rapidly increased RsG in photosynthetic tissue was maintained at a higher level than in controls under both sunlight and Pq, while in non-photosynthetic tissue it gradually decreased with time.

3.2. The effects of sunlight and Pq on antioxidant enzyme activities

The activities of APX, MDAR and GR were higher in non-photosynthetic compared to photosynthetic leaf tissues of dark adapted *P. zonale* plants (Fig. 3). In our previous study, under optimal light conditions, we showed significantly higher activities of APX, DHAR and GR in non-photosynthetic compared to photosynthetic cells (Vidović et al., 2016).

The activity of soluble APX isoforms was strongly stimulated by sunlight in both leaf tissues, particularly in the non-photosynthetic ones. Addition of Pq omitted the light-dependent induction of APX in both tissue types. Furthermore, exposure to sunlight rapidly increased GR activity in both tissues, while Pq suppressed it (Fig. 3, Tables A3, A4). Photosynthetic cells responded to Pq with an abrupt decrease in MDAR, while in non-photosynthetic cells MDAR

activity progressively increased. Under sunlight, DHAR activity gradually increased up to 4 h of exposure in both tissues, while Pq rapidly enhanced DHAR activity, three-fold in photosynthetic and five-fold in non-photosynthetic tissue (Fig. 3, Table A4).

Fig. 3.

As expected, CAT activity was much higher in photosynthetic in comparison to non-photosynthetic tissue (Fig. 4), similar to the results found under optimal light conditions (Vidović et al., 2016), although the difference was less pronounced in dark adapted leaves. The most striking effect of short (1 h) sunlight exposure in photosynthetic tissue of *P. zonale* leaves was a rapid increase of CAT activity in parallel with POD and GR stimulation (Figs. 3, 4; Table A3). In contrast to sunlight exposure, Pq addition increased POD activity only in non-photosynthetic tissue.

Fig. 4.

Both high light and Pq stimulate $O_2^{\bullet-}$ production at PS I, which is rapidly removed by chloroplastic Cu/ZnSOD (Ogawa et al., 1995; Asada, 2000). However, our results showed no significant increase of plastidic Cu/ZnSOD abundance in either cells types under both treatments (Fig. A2).

3.3. H_2O_2 accumulation

In the leaves exposed to high light (HL: 1100 ± 100 μmol m^{-2} s^{-1} PAR), the significant H_2O_2 accumulation (four-fold higher than under growth light, GL: 250 μmol m^{-2} s^{-1} PAR) was restricted to photosynthetic tissue, especially to the tissue along the vascular region (in the case of plain leaf - up to the leaf edge; Fig. 5A). No staining was observed in the leaves incubated only in DAB under growth light, as described previously (Vidović et al., 2016) (Fig. 5C). The same staining pattern as under HL, but more intensive brown coloration indicating higher H_2O_2 accumulation ($P < 0.001$, Mann-Whitney U test) was observed in the leaves incubated with Pq under HL (Fig. 5B). In the leaves exposed to Pq solution under GL, H_2O_2 accumulation was

observed only in the main veins of green leaf area compared to GL (P = 0.017, Mann-Whitney U test) (Fig. 5D).

On the other hand, no H_2O_2 accumulation was observed in non-photosynthetic leaf tissue in any of the treatments. This was confirmed by using different leaf morphotypes (sectorial chimeras and totally white and green leaves; Fig. 5) in order to exclude the differences related to the position of white tissue on the edge of the leaf compared with the center of the leaf.

Fig. 5.

To confirm that H_2O_2 accumulation was related to photosynthetic activity, green leaf areas were kept in the dark during DAB uptake. Only high light-exposed green leaf sectors showed significant H_2O_2 accumulation (Fig. A3).

Under high resolution (40, 100 x magnification), the most intensive coloration was observed in the apoplastic space of vascular tissue followed by surrounding bundle sheet cells, and the lowest in the apoplastic space of mesophyll cells (all in green leaf sectors) (Fig. A4). No staining was observed in epidermal tissue (data not shown).

In order to explore the source of high light-induced H_2O_2 generation in the apoplast, leaves were pre-treated with DPI, an inhibitor of NADPH oxidase responsible for $O_2^{\bullet-}$ production, which is subsequently dismutated to H_2O_2 by extracellular SOD. Application of DPI inhibited H_2O_2 accumulation in vascular and perivascular area (P < 0.001 compared to HL, Mann-Whitney U test), confirming NADPH oxidase-dependent H_2O_2 formation (Fig. 6). The same result was achieved with exogenous CAT application through the leaf petiole (P = 0.006 compared to HL, Mann-Whitney U test), which additionally confirmed that H_2O_2 was accumulated in the apoplastic space of (peri)vascular tissue.

By pre-treating leaves with exogenous (synthetic) 0.1 mM ABA for 1 h (approximately 40 nmol g^{-1}_{FW}) at HL, we wanted to determine whether H_2O_2 accumulated under conditions that induce stomatal closure and limited CO_2 supply. Exogenous ABA uptake inhibited 95% of stomatal conductance in green leaf sectors, and 65% in white ones. However, the distribution and DAB staining intensity were similar to control leaves exposed to HL (Fig. 6).

Fig. 6.

3.4. Stomatal conductance

Under growth light (GL), photosynthetic sectors had higher stomatal conductance compared to the white ones (Table 1; P = 0.001, Mann-Whitney U test). Exposure to high light for 1 h inhibited stomatal conductance (g_s) by 20-30% compared to GL with no differences between the tissue types (Table 1). In comparison, Pq addition under high light (HL) had stronger effect only on photosynthetic cells, decreasing g_s by 35%. Although we detected slight H_2O_2 accumulation in green leaf sectors treated with Pq under GL, the stomatal conductance was unaffected. Interestingly, stomata were not affected by Pq in non-photosynthetic cells under both light regimes.

3.5. ABA distribution

Since we found significant changes in enzyme activities already after the 1st h and apoplastic H_2O_2 accumulation, we measured the ABA concentration in photosynthetic (main veins removed), (peri)vascular and non-photosynthetic tissues to associate its role with early stress response. Under GL, ABA content was almost twice as high in photosynthetic and (peri)vascular tissue than in non-photosynthetic tissue (Table 2; P = 0.010, Mann-Whitney U test). High light rapidly stimulated ABA accumulation in all three leaf areas (5 to 10 times, P < 0.029 Mann-Whitney U test) compared to GL. Under Pq+HL treatment, decreased stomatal conductance in photosynthetic tissue (Table 1) was correlated with ABA accumulation, while in non-photosynthetic tissue we observed only a slight decrease of ABA content. In addition, Pq invoked a decline of ABA content in (peri)vascular tissue (P = 0.029, Mann-Whitney U test; Table 2). Moreover, the sum of the ABA decrease in non-photosynthetic and (peri)vascular tissues (393.4 ng g^{-1}_{FW}, P < 0.029 Mann-Whitney U test) under HL+Pq corresponded to the amount of ABA accumulated in photosynthetic tissue (404.2 ng g^{-1}_{FW}, P < 0.029 Mann-Whitney U test) compared to HL.

4. Discussion

In this study, we showed that, under progressive pro-oxidative conditions induced by strong sunlight and Pq, H_2O_2 significantly accumulated only in illuminated green sectors, and was restricted to the extracellular space of vascular and adjacent photosynthetically active cells (Figs. 5, A3). Similar light-induced H_2O_2 accumulation in the (peri)vascular area has been reported in *Arabidopsis thaliana* and *Mesembryanthemum crystallinum* (Mulineaux et al., 2006; Kuźniak et al., 2016).

The extracellular H_2O_2 accumulation in the (peri)vascular tissue of green leaf segments was additionally confirmed by uptake of exogenous CAT through the leaf petiole, which abolished brown coloration (Fig. 6). Further, we showed that the generation of H_2O_2 was directly dependent on the activity of NADPH oxidase, as evidenced by application of its inhibitor, DPI. Similar findings were reported in maize leaves subjected to osmotic stress (Hu et al., 2006), and in illuminated wheat protoplasts treated with Pq (Robert et al., 2009). Our findings are in line with recent studies indicating that H_2O_2 derived from NADPH oxidase in the apoplast of bundle sheet cells was involved in rapid intercellular signal propagation during acclimatization to high light (Galvez-Valdivieso et al., 2009; Miller et al., 2009; Szechyńska-Hebda et al., 2010; Mittler and Blumwald, 2015). In addition, Fryer et al. (2003) suggested that chloroplasts in bundle sheet cells were more susceptible to H_2O_2 accumulation compared to mesophyll cells under a stimulated Mehler reaction, due to limitations in the CO_2 supply. However, even under decreased stomatal conductance caused by the uptake of exogenous ABA in our study, H_2O_2 accumulation in interveinal leaf sectors did not increase (Fig. 6).

We propose that the absence of H_2O_2 accumulation in mesophyll cells of *P. zonale* leaves under strong sunlight and Pq treatment was the result of efficient antioxidative metabolism in leaf cells. Additional evidence for efficient H_2O_2 scavenging was the absence of APX and chloroplastic Cu/ZnSOD inactivation (Figs. 3, A2). The Cu/ZnSOD is inactivated at 10^{-4} molar concentration of H_2O_2 (Casano et al., 1997), while under conditions of low Asc concentrations, H_2O_2 rapidly inactivates APX activity (Kitajima et al., 2008; Maruta et al., 2016). Similar results related to Cu/ZnSOD in *P. zonale* were also obtained in sugarcane and Arabidopsis leaves treated with Pq (Chagas et al., 2008; Scarpeci et al., 2008).

Our previous results showed that the main antioxidants in photosynthetic cells were Asc, thylakoid-bound APX and CAT, while in non-photosynthetic cells those were GSH, Asc-GSH

cycle enzymes, and Mn and Cu/Zn SOD (Vidović et al., 2016). Accordingly, sudden exposure to pro-oxidative conditions caused distinctive responses in green and white leaf sectors.

The significant difference between photosynthetic and non-photosynthetic tissue was induction of total ascorbate accumulation by strong sunlight solely in green sectors (Fig. 1), which implies the role of photosynthesis in Asc biosynthesis. Stimulation of Asc biosynthesis by high PAR has already been reported in Arabidopsis (Bartoli et al., 2006), and in photosynthetic cells of *P. zonale* (Vidović et al., 2015). On the other hand, the dynamics of GSH content under strong sunlight was similar, though it was significantly higher in non-photosynthetic compared to photosynthetic tissue over the course of the experiment. We have recently discussed the specific distribution of ascorbate and glutathione in relation to heterotrophic and autotrophic metabolisms in these two tissues (Vidović et al., 2016).

In photosynthetic cells, sudden exposure to sunlight rapidly increased activities of GR and CAT, while activity of soluble APX increased after 4 h (Figs. 4, 5). On the other hand, in non-photosynthetic tissue, induction of soluble APX (constitutively higher in this cell type, and mainly consisted of cytosolic isoform, Vidović et al., 2016), was noted already 1 h after exposure to sunlight. This can be correlated with 2.6-fold higher level of Asc in the cytoplasm of non-photosynthetic cells compared to the photosynthetic ones (Vidović et al., 2016). Although GalLDH abundance was constitutively higher in non-photosynthetic tissue (Vidović et al., 2016), we propose that the level of H_2O_2 was regulated through efficient Asc recycling (unchanged Asc content, increased APX, DHAR and GR activities) rather than Asc biosynthesis. These obviously different, tissue-specific strategies in maintaining ascorbate redox status may be attributed to the non-photosynthetic tissue dependence for ascorbate precursors (glucose, galactose and mannose; Ishikawa and Shigeoka, 2008) deriving from photosynthetic tissue (Vidović et al., 2015).

The fast up-regulation of cytosolic APX isoforms (within 30 min) by excess light has been reported, and it has been associated with decreased GSH/GSSG ratio (Karpinski et al., 1997; Szechyńska-Hebda et al., 2010). The delayed APX induction in photosynthetic cells in our study may be explained by the rapid increase of GSH/GSSG ratio and GR activity under sunlight (Fig. 2). This immediate and efficient reduction of GSSG, only in photosynthetic tissue, was dependent on reducing equivalents (NADPH) produced at PS I (Foyer and Noctor, 2011). Besides its widely accepted role in Asc-GSH cycle, GR may participate in the "fine tuning" of

H_2O_2-iniciated intra- and intercellular signaling pathways by modulating GSH/GSSG ratio (Mhamdi et al., 2010; Queval et al., 2011; Han et al., 2013).

The different responses in photosynthetic tissue under sunlight and Pq exposure could be explained by different sites and rates of H_2O_2 generation, as well as different distribution of H_2O_2 scavenging enzymes. Accordingly, Sewelam and co-workers (2014) showed that H_2O_2 produced in peroxisomes induced transcripts involved in protein repair responses, while H_2O_2 produced in chloroplasts provoked early signaling response and mitochondrial retrograde regulation.

The absence of ascorbate accumulation under Pq treatment in photosynthetic tissue can be attributed to abolished ferredoxin photoreduction, an inevitable consequence of Pq treatment (Veljović-Jovanović, 1998; Asada, 2000; Yabuta et al., 2007). However, in non-photosynthetic tissue exposed to Pq the content of Asc increased after 1 h, presumably through its efficient recycling by enhanced MDAR and DHAR activities (Figs. 1, 3). Additionally, rapidly stimulated DHAR activity in photosynthetic cells, together with progressively increasing GR activity (Fig. 3) might be responsible for maintaining high redox state of ascorbate (Fig. 1), when Asc biosynthesis was omitted by Pq. The importance of DHAR in defense against Pq-provoked oxidative stress was demonstrated by higher tolerance of transformed tobacco plants over-expressing DHAR compared to *wt* and plants overexpressing chloroplastic APX and CAT (Lee et al., 2007). The absence of increased APX activity after Pq addition under sunlight in photosynthetic cells might be attributed to a Pq-induced lower plastoquinone redox state. High reduced plastoquinone state is required for triggering APX induction, as it was confirmed by using DCMU (Karpiński et al., 1997; Szechyńska-Hebda et al., 2010). Moreover, in the maize leaves treated with 50 µM Pq for 24 h, APX activity declined (Ding et al., 2009).

Although enhanced generation of H_2O_2 under Pq treatment induced rapid Asc oxidation and monodehydroascorbyl radical formation in detached leaf (Veljović-Jovanović et al., 1998), we obtained gradual increase of MDAR in non-photosynthetic tissue under Pq, but not in the photosynthetic one. Moreover, dynamics of MDAR activity was correlated with POD activity (maximal values after 4 h). Sakihama et al. (2000) showed that MDAR can reduce phenoxyl radicals (such as quercetin radicals), generated by POD and H_2O_2. In our previous study we showed that kaempferol and quercetin in non-photosynthetic cells accumulated under high light (Vidović et al., 2015). Furthermore, high POD activity in this cell type might be correlated to 60% higher volume of vacuole (Vidović et al., 2016), and significantly higher content of

endogenous POD co-substrates, such as *p*-coumaric acid and epicatechin compared to photosynthetic tissue (Vidović et al., 2015). Thus, we propose that in non-photosynthetic cells, which constitutively had lower ascorbate content, MDAR and POD were coupled with phenolic recycling.

Despite the absence of functional chloroplasts in mesophyll cells, guard cells of non-photosynthetic sectors of *P. zonale* leaves contain chloroplasts (Veljović-Jovanović et al., 2016), as observed in white sectors of variegated *Chlorophytum comosum* (Roelfsema et al., 2006). Under growth, light stomatal conductance was higher in green compared to white leaf sectors (Table 1), similarly as in other variegated species, *Hedera helix* and *Chlorophytum comosum* (Aphalo and Sánchez, 1986; Niewiadomska and Miszalski, 1995). However, the stomatal density and pore length were similar in both tissue types of *P. zonale* leaves (Veljović-Jovanović et al., 2016). Under growth light, endogenous ABA content was two times lower in non-photosynthetic leaf tissue than in the photosynthetic tissue, which is in line with white leaves of maize mutant, *vp5* (Hu et al., 2012). High light induced 5-10 times higher ABA content in the whole leaf, but significant stomatal closure only in green sectors (Tables 1, 2). The relationship between ABA (endogenous and exogenous) and stomatal conductance in the plain Pelargonium leaves has recently been confirmed by Boyle et al. (2016). ABA accumulation and localization caused by high light and Pq, (the highest amount in photosynthetic tissue) was not correlated with H_2O_2 distribution (the highest accumulation in (peri)vascular tissue). On the other hand, the involvement of ABA in systemic response to high light has been shown (Mittler and Blumwald, 2015). According to unchanged level of total leaf ABA and the similar amounts of ABA which were reduced in non-photosynthetic and (peri)vascular tissue, and increased in photosynthetic tissue after Pq addition, we can assume that Pq provoked re-distribution of ABA from vascular and non-photosynthetic tissue to the rest photosynthetic tissue (Table 2). Increase of ABA in the photosynthetic mesophyll cells might be a part of protection strategy, since exogenously applied ABA alleviated Pq-induced oxidative damage in maize leaves (Ding et al., 2009). However, the Pq treatment during 12 h did not affect the content of total leaf ABA content in maize during the experimental period (Jiang and Zhang, 2002).

Abrupt and transient changes in antioxidative enzymes' activities in non-photosynthetic cells under strong sunlight and Pq could be triggered by an unknown signal from photosynthetic tissue. For example, Petrillo et al. (2014) described that signals from chloroplasts can be

transduced to roots involving certain redox sensitive protein kinases. However, according to the obtained antioxidative response and the complete absence of H_2O_2 accumulation, we hypothesize that non-photosynthetic leaf tissue may also have an individual response to progressive pro-oxidative conditions, independently from photosynthetic tissue.

Conclusion

Comparison of the antioxidative changes induced by strong sunlight and Pq in two cell types of variegated Pelargonium leaf indicate that both tissues possessed the efficient Asc-GSH cycle able to maintain redox homeostasis during the first hours under stress. In addition, CAT activity in photosynthetic tissue contributed to efficient H_2O_2 scavenging, while in the non-photosynthetic tissue this was attributed to increased PODs activity. Although enzymes of Asc-GSH cycle (APX, DHAR and GR) and total glutathione pool were constitutively higher in non-photosynthetic tissue, under progressive pro-oxidative conditions the reduction of oxidized glutathione was more efficient in photosynthetic tissue, emphasizing the role of photosynthetically-derived reducing equivalents. We suggest that the unexpectedly strong response in non-photosynthetically active tissue could be triggered by the signals from photosynthetic one, but not through extracellular H_2O_2 dependent on NADPH oxidase activity. On the other hand, it is possible that non-photosynthetic tissue responded independently, which could be supported by earlier/higher response of APX to sunlight, and MDAR, DHAR and POD to Pq. Thus, investigating long-distance signaling between photosynthetic and non-photosynthetic tissue and the possibility of independent signal generation in non-photosynthetic tissue should be a goal in the future studies using this model system.

Acknowledgments

This work was supported by the Ministry of Education, Science and Technological Development, Republic of Serbia (Project No. III43010). The authors would like to thank Dr. Ivan Spasojevic (IMSI, University of Belgrade, Serbia) for useful discussion. The authors would like to thank Dr. Ana Vuleta (IBISS, Belgrade University, Serbia) for help with SOD gel blot analysis.

References

Aphalo, P.J., Sanchez, R.A., 1986. Stomatal responses to light and drought stress in variegated leaves of *Hedera helix*. Plant Physiol. 81, 768–773.

Asada, K., 2000. The water–water cycle as alternative photon and electron sinks. Philos. Trans. R. Soc. Lond., B, Biol. Sci. 355, 1419−1431.

Asada, K., 2006. Production and scavenging of reactive oxygen species in chloroplasts and their functions. Plant Physiol. 141, 391–396.

Bartoli, C.G., Yu, J., Gómez, F., Fernández, L., McIntosh, L., Foyer, C.H., 2006. Inter-relationships between light and respiration in the control of ascorbic acid synthesis and accumulation in *Arabidopsis thaliana* leaves. J. Exp. Bot. 57, 1621–1631.

Boyle, R.K., McAinsh, M., Dodd, I.C., 2016. Stomatal closure of *Pelargonium*× *hortorum* in response to soil water deficit is associated with decreased leaf water potential only under rapid soil drying. Physiol Plant. 156, 84-96.

Casano, L.M., Gómez, L.D., Lascano, H.R., González, C.A., Trippi, V.S., 1997. Inactivation and Degradation of CuZn-SOD by Active Oxygen Species in Wheat Chloroplasts Exposed to Photooxidative Stress. Plant Cell Physiol. 38, 433–440.

Chagas, R.M., Silveira, J.A., Ribeiro, R.V., Vitorello, V.A., Carrer, H., 2008. Photochemical damage and comparative performance of superoxide dismutase and ascorbate peroxidase in sugarcane leaves exposed to paraquat-induced oxidative stress. Pestic Biochem Physiol. 90, 181–188.

Cochemé, H.M., Murphy, M.P., 2008. Complex I is the major site of mitochondrial superoxide production by paraquat. J. Biol. Chem. 283, 1786–1798.

Ding, H.D., Zhang, X.H., Xu, S.C., Sun, L.L., Jiang, M.Y., Zhang, A., Jin, Y. G., 2009. Induction of protection against paraquat-induced oxidative damage by abscisic acid in maize leaves is mediated through mitogen-activated protein kinase. J. Integr. Plant Biol. 51, 961–972.

Foyer, C.H., Noctor, G., 2011. Ascorbate and glutathione: the heart of the redox hub. Plant Physiol. 155, 2–18.

Foyer, C.H., Shigeoka S., 2011. Understanding oxidative stress and antioxidant functions to enhance photosynthesis. Plant Physiol. 155, 93–100.

Fryer, M.J., Ball, L., Oxborough, K., Karpiński, S., Mullineaux, P.M., Baker, N.R., 2003. Control of *Ascorbate Peroxidase 2* expression by hydrogen peroxide and leaf water status during excess light stress reveals a functional organisation of *Arabidopsis* leaves. Plant J. 33, 691–705.

Galvez-Valdivieso, G., Fryer, M.J., Lawson, T., Slattery, K., Truman, W., Smirnoff, N., et al., 2009. The high light response in *Arabidopsis* involves ABA signaling between vascular and bundle sheath cells. Plant Cell 21, 2143–2162.

Han, Y., Chaouch, S., Mhamdi, A., Queval, G., Zechmann, B., Noctor, G., 2013. Functional analysis of Arabidopsis mutants points to novel roles for glutathione in coupling H_2O_2 to activation of salicylic acid accumulation and signaling. Antioxid. Redox Signal. 18, 2106–2121.

Hu, X., Zhang, A., Zhang, J., Jiang, M., 2006. Abscisic acid is a key inducer of hydrogen peroxide production in leaves of maize plants exposed to water stress. Plant Cell Physiol. 47, 1484–1495.

Hu, X., Wu, X., Li, C., Lu, M., Liu, T., Wang, Y., et al., 2012. Abscisic acid refines the synthesis of chloroplast proteins in maize (*Zea mays*) in response to drought and light. PloS ONE 7, e49500.

Ishikawa, T., Shigeoka, S., 2008. Recent advances in ascorbate biosynthesis and the physiological significance of ascorbate peroxidase in photosynthesizing organisms. Biosci. Biotechnol. Biochem. 72, 1143–1154.

Jiang, M., Zhang, J., 2002. Water stress-induced abscisic acid accumulation triggers the increased generation of reactive oxygen species and up-regulates the activities of antioxidant enzymes in maize leaves. J. Exp. Bot. 53, 2401–2410.

Kangasjärvi, S., Lepistö, A., Hännikäinen, K., Piippo, M., Luomala, E.M., Aro, E.M., 2008. Diverse roles for chloroplast stromal and thylakoid bound ascorbate peroxidases in plant stress responses. Biochem. J. 412, 275–285.

Karpiński, S., Escobar, C., Karpinska, B., Creissen, G., Mullineaux, P.M., 1997. Photosynthetic electron transport regulates the expression of cytosolic ascorbate peroxidase genes in Arabidopsis during excess light stress. Plant Cell 9, 627–640.

Kitajima, S., Kurioka, M., Yoshimoto, T., Shindo, M., Kanaori, K., Tajima, K., et al., 2008. A cysteine residue near the propionate side chain of heme is the radical site in ascorbate peroxidase. FEBS J. 275, 470–480.

Kuźniak, E., Kornas, A., Kaźmierczak, A., Rozpądek, P., Nosek, M., Kocurek, M., et al., 2016. Photosynthesis-related characteristics of the midrib and the interveinal lamina in leaves of the C3-CAM intermediate plant *Mesembryanthemum crystallinum*. Ann. Bot. 117, 1141-1151.

Lascano, R., Quero, G., Robert, G., Melchiorre, M., Rodriguez, M., Muñoz, N., et al., 2012. Paraquat: an oxidative stress inducer. In: Hasaneen, M.N. (Ed.), Herbicides-Properties, Synthesis and Control of Weeds. InTech, Rijeka, Croatia, pp. 135–148.

Lee, Y.P., Kim, S.H., Bang, J.W., Lee, H.S., Kwak, S.S., Kwon, S.Y., 2007. Enhanced tolerance to oxidative stress in transgenic tobacco plants expressing three antioxidant enzymes in chloroplasts. Plant Cell Rep. 26, 591−598.

Li, J., Mu, J., Bai, J., Fu, F., Zou, T., An, F., et al., 2013. Paraquat Resistant1, a Golgi-localized putative transporter protein, is involved in intracellular transport of paraquat. Plant Physiol. 162, 470−483.

Maruta, T., Sawa, Y., Shigeoka, S., Ishikawa, T., 2016. Diversity and evolution of ascorbate peroxidase functions in chloroplasts: more than just a classical antioxidant enzyme? Plant Cell Physiol. doi: 10.1093/pcp/pcv203.

Mhamdi, A., Hager, J., Chaouch, S., Queval, G., Han, Y., Taconnat, L., et al., 2010. Arabidopsis GLUTATHIONE REDUCTASE1 plays a crucial role in leaf responses to intracellular hydrogen peroxide and in ensuring appropriate gene expression through both salicylic acid and jasmonic acid signaling pathways. Plant Physiol. 153, 1144–1160.

Miller, G., Schlauch, K., Tam, R., Cortes, D., Torres, M.A., Shulaev, V., et al., 2009. The plant NADPH oxidase RBOHD mediates rapid systemic signaling in response to diverse stimuli. Sci Signal 2**,** ra45.

Mittler, R., Blumwald, E., 2015. The roles of ROS and ABA in systemic acquired acclimation. Plant Cell 27, 64−70.

Møller, I.M., 2001. Plant mitochondria and oxidative stress: electron transport, NADPH turnover, and metabolism of reactive oxygen species. Annu. Rev. Plant Physiol. Plant Mol. Biol. 52, 561–591.

Morina, F., Jovanović, L., Prokić, L., Veljović-Jovanović, S., 2016. Physiological basis of differential zinc and copper tolerance of *Verbascum* populations from metal-contaminated and uncontaminated areas. Environ Sci Pollut Res Int doi: 10.1007/s11356-016-6177-4.

Mullineaux, P.M., Karpiński, S., Baker, N.R., 2006. Spatial dependence for hydrogen peroxide-directed signaling in light-stressed plants. Plant Physiol. 141, 346−350.

Neuhaus, H.E., Stitt, M., 1989. Perturbation of photosynthesis in spinach leaf discs by low concentrations of methyl viologen: Influence of increased thylakoid energisation on ATP synthesis, electron transport, energy dissipation, light-activation of the Calvin-cycle enzymes, and control of starch and sucrose synthesis. Planta 179, 51–60.

Niewiadomska, E., Miszalski, Z., 1995. Does CO_2 modify the effect of SO_2 on variegated leaves of *Chlorophytum comosum* (Thunb) Bak? New Phytol. 130, 461-466.

Ogawa, K., Kanematsu, S., Takabe, K., Asada, K., 1995. Attachment of CuZn-superoxide dismutase to thylakoid membranes at the site of superoxide generation (PS I) in spinach chloroplasts: detection by immuno-gold labeling after rapid freezing and substitution method. Plant Cell Physiol. 36, 565–573.

Petrillo, E., Godoy Herz, M.A., Fuchs, A., Reifer, D., Fuller, J., Yanovsky, M.J., et al., 2014. A chloroplast retrograde signal regulates nuclear alternative splicing. Science 344, 427–430.

Robert, G., Melchiorre, M., Racca, R., Trippi, V., Lascano, H.R., 2009. Apoplastic superoxide level in wheat protoplast under photooxidative stress is regulated by chloroplast redox signals: Effects on the antioxidant system. Plant Sci. 177, 168–174.

Roelfsema, M.R., Konrad, K.R., Marten, H., Psaras, G.K., Hartung, W., Hedrich, R., 2006. Guard cells in albino leaf patches do not respond to photosynthetically active radiation, but are sensitive to blue light, CO_2 and abscisic acid. Plant Cell Environ. 29, 1595–1605.

Queval, G., Jaillard, D., Zechmann, B., Noctor, G., 2011. Increased intracellular H_2O_2 availability preferentially drives glutathione accumulation in vacuoles and chloroplasts. Plant Cell Environ. 34, 21–32.

Sakihama, Y., Mano, J., Sano, S., Asada, K., Yamasaki, H., 2000. Reduction of phenoxyl radicals mediated by monodehydroascorbate reductase. Biochem. Biophys. Res. Commun. 279, 949–954.

Scarpeci, T.E., Zanor, M.I., Carrillo, N., Mueller-Roeber, B., Valle, E.M., 2008. Generation of superoxide anion in chloroplasts of *Arabidopsis thaliana* during active photosynthesis: a focus on rapidly induced genes. Plant Mol. Biol. 66, 361−378.

Sewelam, N., Jaspert, N., Van Der Kelen, K., Tognetti, V.B., Schmitz, J., Frerigmann, H., et al., 2014. Spatial H_2O_2 signaling specificity: H_2O_2 from chloroplasts and peroxisomes modulates the plant transcriptome differentially. Mol Plant 7, 1191−1210.

Sierla, M., Rahikainen, M., Salojärvi, J., Kangasjärvi, J., Kangasjärvi, S., 2013. Apoplastic and chloroplastic redox signaling networks in plant stress responses. Antioxid. Redox Signal. 18, 2220–2239.

Stonebloom, S., Brunkard, J.O., Cheung, A.C., Jiang, K., Feldman, L., Zambryski, P., 2012. Redox states of plastids and mitochondria differentially regulate intercellular transport via plasmodesmata. Plant Physiol. 158, 190–199.

Szechyńska-Hebda, M., Kruk, J., Górecka, M., Karpińska, B., Karpiński, S., 2010. Evidence for light wavelength-specific photoelectrophysiological signaling and memory of excess light episodes in Arabidopsis. Plant Cell 22, 2201–2218.

Toshoji, H., Katsumata, T., Takusagawa, M., Yusa, Y., Sakai, A., 2011. Effects of chloroplast dysfunction on mitochondria: white sectors in variegated leaves have higher mitochondrial DNA levels and lower dark respiration rates than green sectors. Protoplasma 249, 805–817.

Veljović-Jovanović, S., 1998. Active oxygen species and photosynthesis: Mehler and ascorbate peroxidase reactions. Iugosl. Physiol. Pharmacol. Acta 34, 503–522.

Veljović-Jovanović, S., Oniki, T., Takahama, U., 1998. Detection of monodehydroascorbic acid radical in sulfite-treated leaves and mechanism of its formation. Plant Cell Physiol. 39, 1203–1208.

Veljović-Jovanović, S., Vidović, M., Morina, F. Prokić, Lj., Todorović D.M., 2016. Comparison of photoacoustic signals in photosynthetic and nonphotosynthetic leaf tissues of variegated *Pelargonium zonale.* Int J Thermophys 37: 91, doi: 10.1007/s10765-016-2092-7.

Vicente, J.A., Peixoto, F., Lopes, M.L., Madeira, V., 2001. Differential sensitivities of plant and animal mitochondria to the herbicide paraquat. J. Biochem. Mol. Toxicol. 15, 322–330.

Vidović, M., Morina, F., Milić, S., Albert, A., Zechmann, B., Tosti, T. et al., 2015. Carbon allocation from source to sink leaf tissue in relation to flavonoid biosynthesis in variegated *Pelargonium zonale* under UV-B radiation and high PAR intensity. Plant Physiol. Biochem. 93, 44–55.

Vidović, M., Morina, F., Milić, S., Vuleta, A., Zechmann, B., Prokić, L. et al., 2016. Characterisation of antioxidants in photosynthetic and non-photosynthetic leaf tissues of variegated *Pelargonium zonale* plants. Plant Biol (Stuttg) 18, 669–680.

Yabuta, Y., Mieda, T., Rapolu, M., Nakamura, A., Motoki, T., Maruta, T., et al., 2007. Light regulation of ascorbate biosynthesis is dependent on the photosynthetic electron transport chain but independent of sugars in Arabidopsis. J. Exp. Bot. 58, 2661–2671.

Figure captions

Figure 1. Ascorbate pool in photosynthetic (black) and non-photosynthetic tissue (white) of *P. zonale* leaves during 9 h exposure to direct solar radiation in water (squares) and in 100 µM Pq solution (triangles). Bars show standard errors (n = 5). Significant differences between photosynthetic and non-photosynthetic leaf tissue according to the Mann-Whitney U test are indicated ($^{*}P < 0.05$, $^{**}P < 0.01$). C-control: photosynthetic and non-photosynthetic tissues of dark adapted leaves.

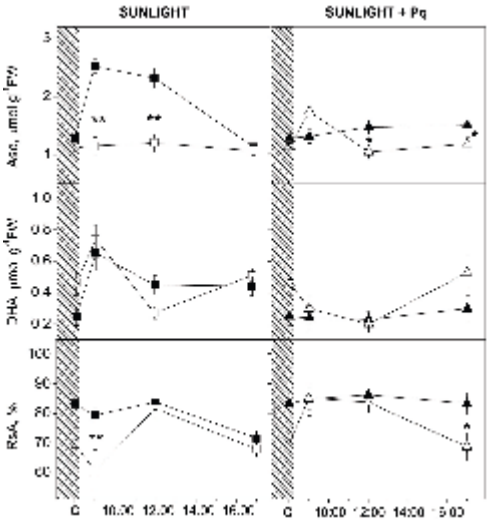

Figure 2. Glutathione pool in photosynthetic (black) and non-photosynthetic tissue (white) of *P. zonale* leaves during 9 h exposure to direct solar radiation in water (squares) and in 100 µM Pq solution (triangles). Bars show standard errors (n = 4). Significant differences between photosynthetic and non-photosynthetic leaf tissue according to the Mann-Whitney U test are indicated ($^{*}P < 0.05$). C-control: photosynthetic and non-photosynthetic tissues of dark adapted leaves.

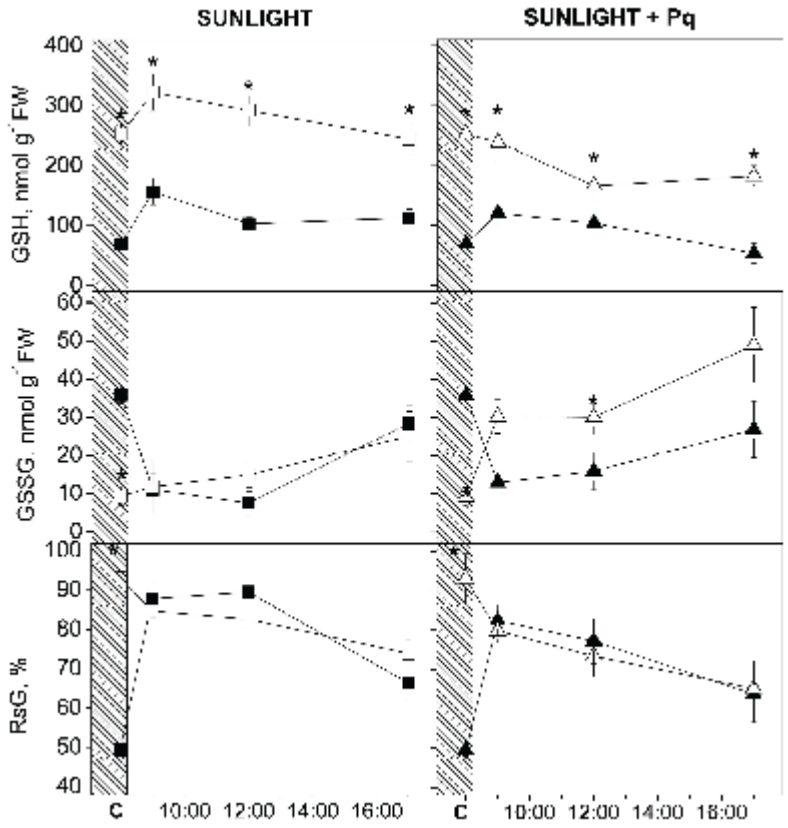

Figure 3. Specific activities (U mg^{-1}) of Asc-GSH cycle enzymes in photosynthetic (black) and non-photosynthetic tissue (white) of *P. zonale* leaves during 9 h exposure to direct solar radiation in water (squares) and in 100 µM Pq solution (triangles). Bars show standard errors (n = 4-5). Significant differences between photosynthetic and non-photosynthetic leaf tissue according to the Mann-Whitney U test are indicated ($^{*}P < 0.05$, $^{**}P < 0.01$). C-control: photosynthetic and non-photosynthetic tissues of dark adapted leaves.

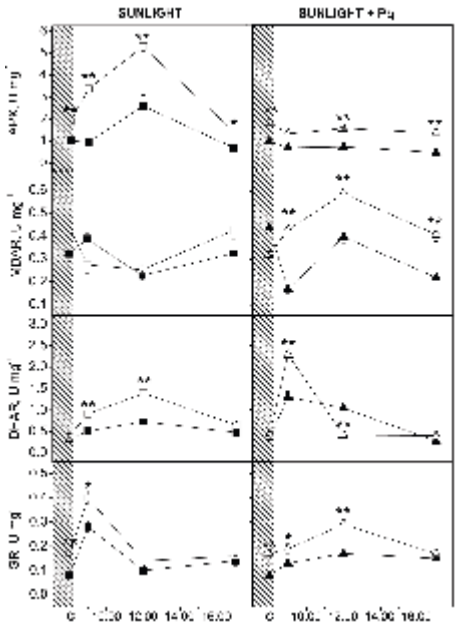

Figure 4. Specific activities (U mg^{-1}) of CAT and POD in photosynthetic (black) and non-photosynthetic tissue (white) of *P. zonale* leaves during 9 h exposure to direct solar radiation in water (squares) and in 100 µM Pq solution (triangles). Bars show standard errors (n = 4-5). Significant differences between photosynthetic and non-photosynthetic leaf tissue according to the Mann-Whitney U test are indicated ($^{*}P < 0.05$, $^{**}P < 0.01$). C-control: photosynthetic and non-photosynthetic tissues of dark adapted leaves.

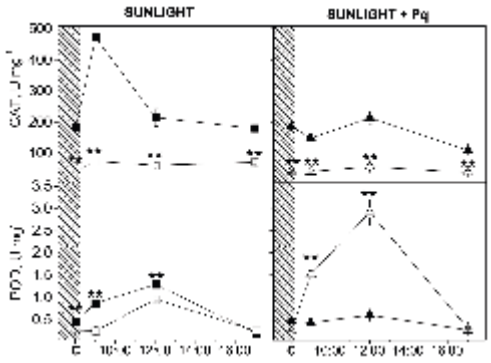

Figure 5. Accumulation of H_2O_2 in *P. zonale* leaves detected by DAB 'up-take': A) after 1 h under high light (HL); B) after 1 h under 100 µM Pq + HL; C) after 2.5 h under growth light (GL); D) after 2.5 h under 100 µM Pq + GL (enough time to achieve equal uptake of Pq and DAB as under HL). Each leaf was photographed before and after chlorophyll removal. Hydrogen peroxide was visualized as brown coloration and the staining intensity presented in arbitrary units: HL, 28.5 ± 1.5; HL+Pq, 45.0 ± 4.1; GL, 7.7 ± 2.4; GL+Pq, 17.8 ± 1.2 (values present means ± SE, n = 15).

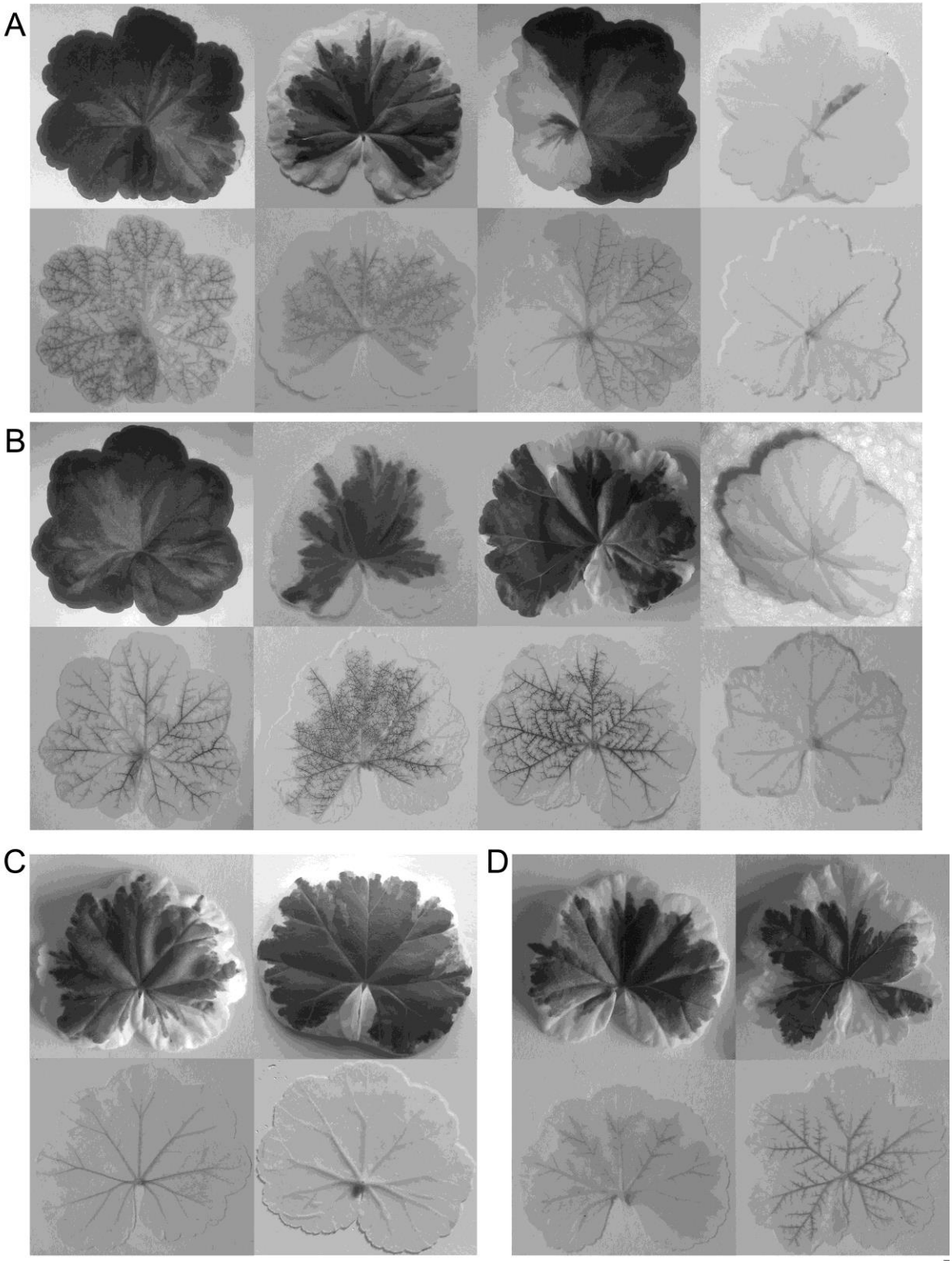

Figure 6. Differential accumulation of H_2O_2 in leaves pre-treated with NADPH oxidase inhibitor (0.1 mM DPI), 50 U CAT, 0.1 mM ABA and exposed to strong sunlight for 1 h. Hydrogen

peroxide was visualized as brown coloration and the staining intensity presented in arbitrary units: DPI, 4.8 ± 1.8; CAT, 7.1 ± 0.8; ABA, 36.2 ± 4.5 (values present means ± SE, n = 7).

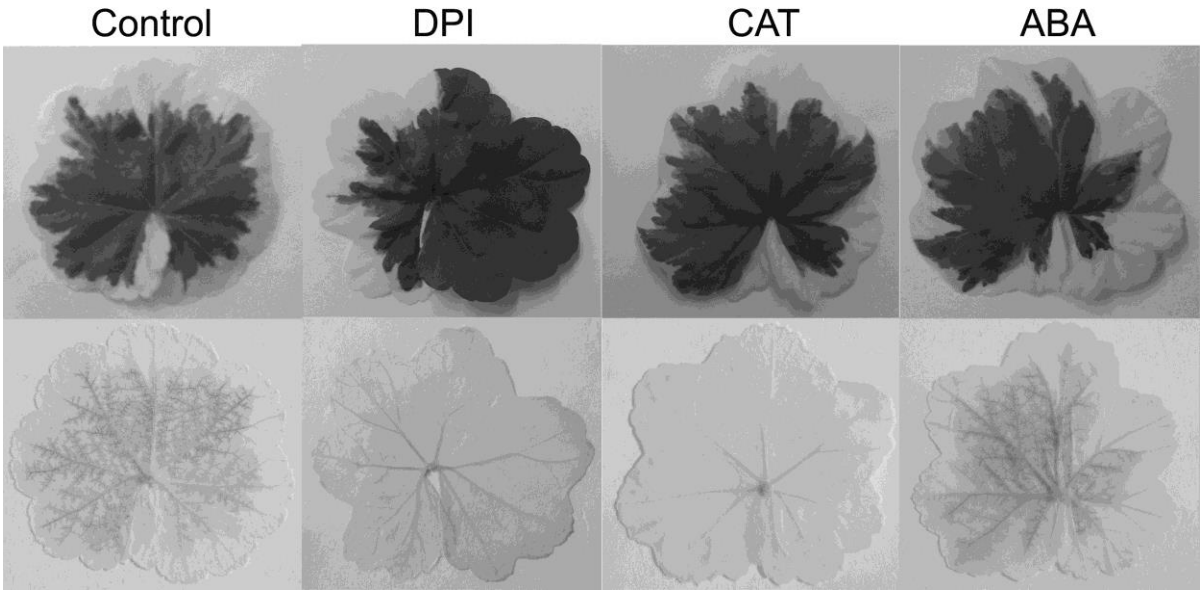

Appendix A

Figure A1. Temperature (T, ºC) and radiation conditions (PAR, µmol m^{-2} s^{-1}, UV-A and UV-B irradiance, W m^{-2}) at the leaf level, during the representative experiment in June 2011.

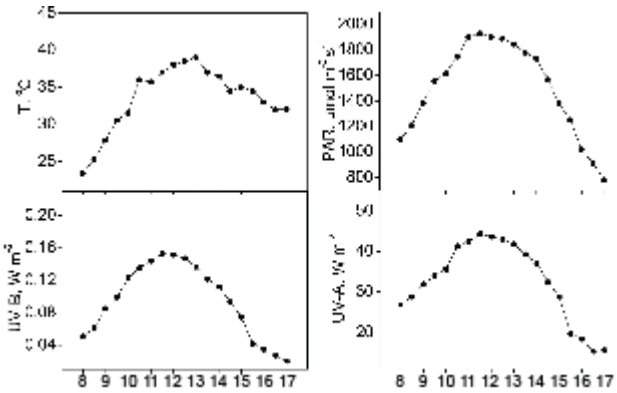

Figure A2. Dynamics of Cu/ZnSOD response in green (G), and white (W) sectors of *P. zonale* leaves after 1 h and 4 h exposure to direct solar radiation and 100 µM Pq solution. Blot analysis (15% PAG) of Cu/ZnSOD showing two immunoreactive bands (Mm 16 and 18 kDa (Vidović *et al*., 2015) indicated by arrows. C-control: dark adapted leaves. Seven µg of proteins were applied to each well, equal loading was confirmed by staining the replicate gels with silver. Numbers represent relative amounts of SOD in percentages (means, n = 3, errors were less than 10%),

estimated by determining band volume using Optimas 6.5.1 (Media Cybernetics Inc., Bethesda, MD, USA).

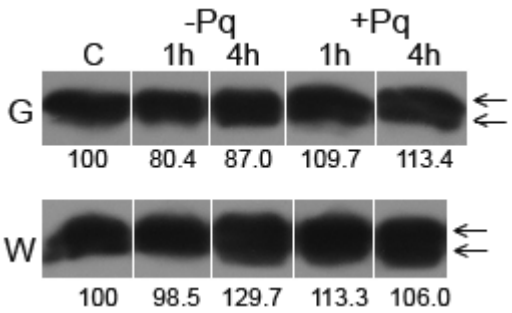

Figure A3. DAB staining of H_2O_2 in leaves exposed to strong sunlight (>1100 µmol m^{-2} s^{-1} PAR) for 1 h followed by incubation in buffer without DAB. A) The lateral and bottom leaf halves were kept in the dark; B) leaves were incubated in 100 µM Pq, while lateral leaf halves were kept in the dark; C) random leaf areas (circles) were exposed to strong sunlight.

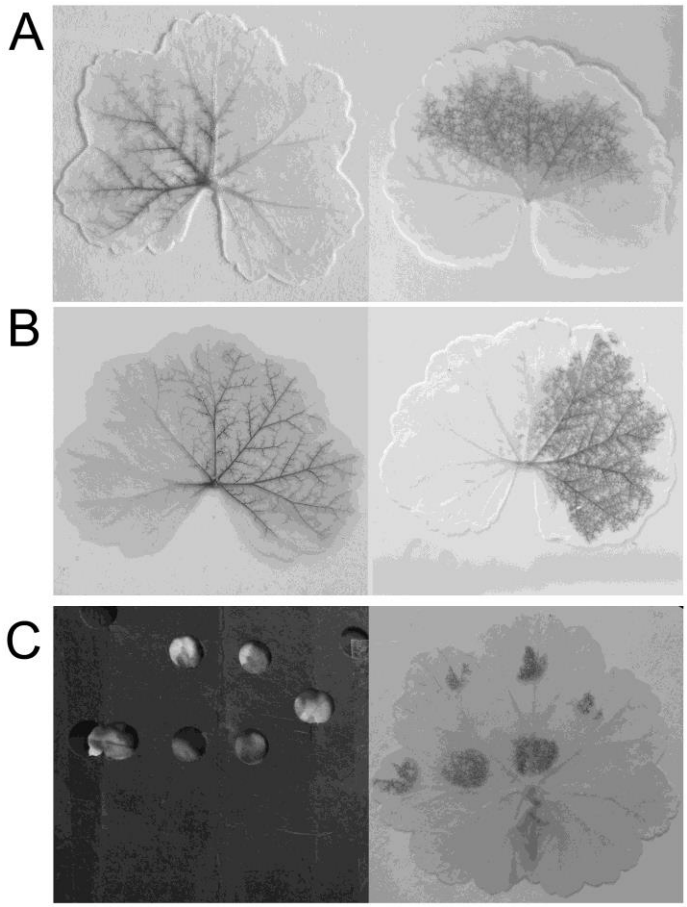

Figure A4. Histochemical detection of H_2O_2 in *P. zonale* leaves after 1 h exposure to high light by 'DAB up-take' method. A) Junction between green and white leaf sector, 2x magnification

(bar represents 2.5 mm); B) the same leaf area 5x magnified (bar represents 1 mm); C) longitudinal section of green (peri)vascular tissue (40x, bar represents 100µm), and D) cross section of green leaf (peri)vascular tissue (100x, bar represents 50µm).

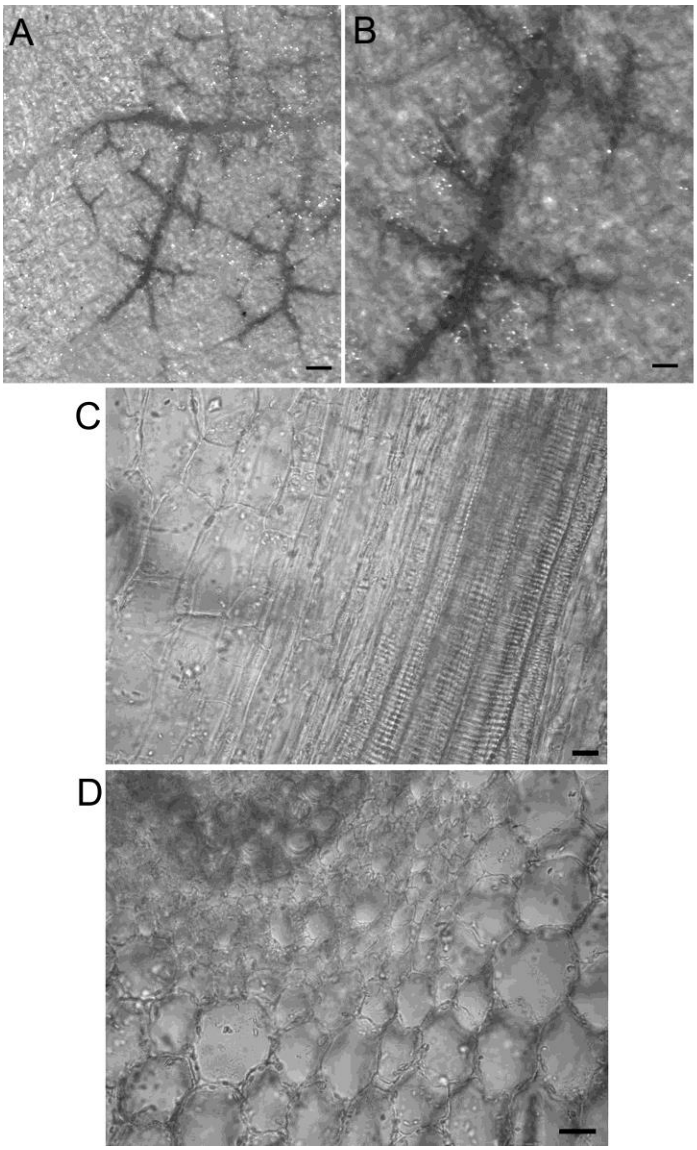

Table 1. Stomatal conductance (g_s, mmol m^{-2} s^{-1} PAR in photosynthetic and non-photosynthetic leaf tissue under growth light (GL, 250 µmol m^{-2} s^{-1} PAR) with and without 100 µM Pq (GL+Pq), and after 1 h of exposure to high light (HL, 1100 ± 100 µmol m^{-2} s^{-1} PAR) and 100 µM Pq (HL+Pq). Values represent means ± SE and different letters denote statistically significant differences between different treatments for each tissue type ($P < 0.05$) (n = 10).

	GL	GL+Pq	HL	HL+Pq
photosynthetic tissue	579.7 ± 77.8 ^{b}	580.9 ± 22.2 ^{b}	393.9 ± 22.6 ^{ab}	149.0 ± 47.0 ^{a}
non-photosynthetic tissue	158.5 ± 19.7 ^{a}	120.5 ± 16.9 ^{a}	125.0 ± 12.6 ^{a}	94.1 ± 24.5 ^{a}

Table 2. ABA content (ng g^{-1}_{FW}) in photosynthetic (without main veins), vascular and non-photosynthetic tissue, in dark adapted leaves and after 1 h of exposure to growth light (GL, 250 µmol m^{-2} s^{-1} PAR), high light (HL, 1100 ± 100 µmol m^{-2} s^{-1} PAR), and 100 µM Pq under HL (HL+Pq). Values represent means ± SE and different letters denote statistically significant differences between different treatments for each tissue type ($P < 0.05$) (n > 6).

	Dark	GL	HL	HL+Pq
photosynthetic tissue	83.1 ± 18.6 ^{a}	96.7 ± 25.8 ^{a}	537.8 ± 66.2 ^{b}	942.0 ± 144.4 ^{c}
(peri)vascular tissue	72.8 ± 19.0 ^{a}	92.4 ± 17.2 ^{a}	442.2 ± 75.7 ^{b}	241.0 ± 16.6 ^{a}
non-photosynthetic tissue	44.2 ± 14.0 ^{a}	39.8 ± 2.4 ^{a}	406.6 ± 105.8 ^{b}	265.1 ± 23.9 ^{ab}

Table A1. Significant differences in ascorbate pool between dark adapted leaves, 1-, 4- and 9-h period of exposure to sunlight and 100 µM Pq according to the Mann-Whitney U test. The *P*-values for photosynthetic and non-photosynthetic tissue are reported and bolded when significant differences were detected ($P < 0.05$). C, control (dark adapted leaves).

Sunlight

Photosynthetic tissue

Asc	C	1	4	9
C		**0.008**	**0.008**	0.421
1	-		0.310	**0.008**
4	-	-		**0.008**
9	-	-	-	
DHA	C	1	4	9
C		**0.008**	0.095	0.095
1	-		0.310	0.310
4	-	-		1.000
9	-	-	-	

Non-photosynthetic tissue

Asc	C	1	4	9
C		1.000	0.548	0.421
1	-		1.000	1.000
4	-	-		0.548
9	-	-	-	
DHA	C	1	4	9
C		0.056	0.222	1.000
1	-		**0.008**	**0.032**
4	-	-		**0.008**
9	-	-	-	

RsA	C	1	4	9
C		0.548	0.841	**0.016**
1	-		0.548	0.095
4	-	-		**0.032**
9	-	-	-	

RsA	C	1	4	9
C		0.310	0.310	0.548
1	-		**0.008**	0.548
4	-	-		**0.032**
9	-	-	-	

Sunlight + Pq

Asc	C	1	4	9
C		1.000	0.151	0.222
1	-		0.548	0.151
4	-	-		1.000
9	-	-	-	

Asc	C	1	4	9
C		**0.008**	0.548	0.310
1	-		**0.008**	**0.008**
4	-	-		0.841
9	-	-	-	

DHA	C	1	4	9
C		1.000	0.841	0.690
1	-		1.000	0.690
4	-	-		0.548
9	-	-	-	

DHA	C	1	4	9
C		0.222	0.056	0.690
1	-		0.421	0.151
4	-	-		**0.016**
9	-	-	-	

RsA	C	1	4	9
C		1.000	0.310	1.000
1	-		0.841	1.000
4	-	-		0.548
9	-	-	-	

RsA	C	1	4	9
C		0.095	**0.032**	1.000
1	-		1.000	0.056
4	-	-		0.095
9	-	-	-	

Table A2. Significant differences in glutathione pool between dark adapted leaves, 1-, 4- and 9-h period of exposure to sunlight and 100 µM Pq according to the Mann-Whitney U test. The *P*-values for photosynthetic and non-photosynthetic tissue are reported and bolded when significant differences were detected ($P < 0.05$). C, control (dark adapted leaves).

Sunlight

Photosynthetic tissue

GSH	C	1	4	9
C		**0.029**	0.057	0.200
1	-		0.057	0.200
4	-	-		0.686
9	-	-	-	

GSSG	C	1	4	9
C		**0.029**	0.200	0.486
1	-		**0.029**	0.057
4	-	-		0.886
9	-	-	-	

Non-photosynthetic tissue

GSH	C	1	4	9
C		0.200	0.343	0.343
1	-		0.114	0.057
4	-	-		0.057
9	-	-	-	

GSSG	C	1	4	9
C		1.000	0.343	0.057
1	-		0.686	0.200
4	-	-		0.343
9	-	-	-	

RsG	C	1	4	9
C		**0.029**	**0.029**	**0.029**
1	-		**0.029**	0.057
4	-	-		0.686
9	-	-	-	

RsG	C	1	4	9
C		**0.029**	**0.029**	**0.029**
1	-		0.343	**0.029**
4	-	-		**0.029**
9	-	-	-	

Sunlight + Pq

GSH	C	1	4	9
C		**0.029**	**0.029**	0.486
1	-		0.686	0.343
4	-	-		0.886
9	-	-	-	

GSH	C	1	4	9
C		1.000	0.057	0.057
1	-		0.200	0.200
4	-	-		0.486
9	-	-	-	

GSSG	C	1	4	9
C		**0.029**	**0.029**	0.686
1	-		0.686	0.343
4	-	-		0.343
9	-	-	-	

GSSG	C	1	4	9
C		**0.029**	**0.029**	**0.029**
1	-		1.000	**0.029**
4	-	-		**0.029**
9	-	-	-	

RsG	C	1	4	9
C		**0.029**	**0.029**	0.686
1	-		0.886	0.200
4	-	-		0.343
9	-	-	-	

RsG	C	1	4	9
C		**0.029**	**0.029**	**0.029**
1	-		0.200	**0.029**
4	-	-		0.486
9	-	-	-	

Table A3. Significant differences in antioxidative enzymes activities between dark adapted leaves, 1-, 4- and 9-h period of exposure to sunlight according to the Mann-Whitney U test. The *P*-values for photosynthetic and non-photosynthetic leaf tissues are reported and bolded when significant differences were detected ($P < 0.05$). C, control (dark adapted leaves). Other abbreviations are explained in Table 4.

Sunlight

Photosynthetic tissue

APX	C	1	4	9
C		0.548	0.160	0.095
1	-		**0.016**	0.222
4	-	-		**0.008**
9	-	-	-	

MDAR	C	1	4	9
C		0.095	**0.032**	0.841
1	-		**0.008**	0.421
4	-	-		0.098
9	-	-	-	

Non-photosynthetic tissue

APX	C	1	4	9
C		**0.008**	**0.008**	0.548
1	-		**0.008**	**0.008**
4	-			**0.008**
9	-	-	-	

MDAR	C	1	4	9
C		**0.016**	**0.008**	0.690
1	-		0.548	**0.032**
4	-	-		**0.008**
9	-	-	-	

DHAR	C	1	4	9
C		**0.032**	**0.008**	**0.032**
1	-		0.056	0.690
4	-	-		0.056
9	-	-	-	

DHAR	C	1	4	9
C		**0.008**	**0.008**	**0.016**
1	-		**0.016**	0.056
4	-			**0.016**
9	-	-	-	

GR	C	1	4	9
C		**0.008**	0.095	**0.016**
1	-		**0.008**	**0.008**
4	-	-		0.095
9	-	-	-	

GR	C	1	4	9
C		**0.008**	0.056	0.690
1	-		**0.008**	**0.008**
4	-			0.421
9	-	-	-	

POD	C	1	4	9
C		**0.008**	0.421	1.000
1	-		**0.008**	**0.008**
4	-	-		0.421
9	-	-	-	

POD	C	1	4	9
C		**0.032**	0.056	0.056
1	-		0.222	1.000
4	-			0.421
9	-	-	-	

CAT	C	1	4	9
C		**0.008**	**0.008**	**0.008**
1	-		**0.008**	**0.008**
4	-	-		**0.008**
9	-	-	-	

CAT	C	1	4	9
C		0.548	**0.008**	1.000
1	-		**0.008**	1.000
4	-			**0.008**
9	-	-	-	

Table A4. Significant differences in antioxidative enzymes activities between dark adapted leaves, 1-, 4- and 9-h period of incubation in 100 µM Pq according to the Mann-Whitney U test. The *P*-values for photosynthetic and non-photosynthetic leaf tissues are reported and bolded when significant differences were detected ($P < 0.05$). C, control (dark adapted leaves). Other abbreviations are explained in Table 4.

Sunlight + Pq

Photosynthetic tissue

APX	C	1	4	9
C		0.310	**0.016**	**0.008**
1	-		0.690	0.548
4	-	-		0.095
9	-	-	-	

MDAR	C	1	4	9
C		**0.008**	0.151	**0.008**
1	-		**0.008**	0.222
4	-	-		**0.008**

Non-photosynthetic tissue

APX	C	1	4	9
C		**0.032**	0.151	0.056
1	-		0.151	0.841
4	-	-		0.421
9	-	-	-	

MDAR	C	1	4	9
C		0.841	**0.032**	0.690
1	-		**0.032**	1.000
4	-	-		**0.016**

9	-	-	-	

DHAR	C	1	4	9
C		**0.008**	**0.008**	0.222
1	-		0.222	**0.008**
4	-	-		**0.008**
9	-	-	-	

GR	C	1	4	9
C		**0.016**	**0.008**	**0.008**
1	-		0.095	0.548
4	-	-		0.222
9	-	-	-	

POD	C	1	4	9
C		**0.032**	0.310	**0.008**
1	-		0.056	**0.032**
4	-	-		**0.008**
9	-	-	-	

CAT	C	1	4	9
C		0.690	**0.032**	**0.032**
1	-		0.151	0.056
4	-	-		**0.008**
9	-	-	-	

9	-	-	-	

DHAR	C	1	4	9
C		**0.008**	1.000	0.841
1	-		**0.008**	**0.008**
4	-	-		0.841
9	-	-	-	

GR	C	1	4	9
C		0.690	**0.008**	0.548
1	-		**0.032**	0.222
4	-	-		**0.008**
9	-	-	-	

POD	C	1	4	9
C		**0.008**	**0.008**	0.421
1	-		**0.008**	**0.008**
4	-	-		**0.008**
9	-	-	-	

CAT	C	1	4	9
C		0.548	0.095	0.548
1	-		0.548	0.690
4	-	-		0.222
9	-	-	-	